# Carbon Nanotube–Loaded Nafion Film Electrochemical Sensor for Metal Ions: Europium

**6 AUTHORS**, INCLUDING:

Tingting Wang
University of Texas at Austin
**14** PUBLICATIONS **61** CITATIONS

SEE PROFILE

Bill L. Riehl
BlackFire Engineering Ltd
**13** PUBLICATIONS **132** CITATIONS

SEE PROFILE

# Carbon Nanotube-Loaded Nafion Film Electrochemical Sensor for Metal Ions: Europium

Tingting Wang,[†] Daoli Zhao,[†] Xuefei Guo,[†] Jaime Correa,[†] Bill L. Riehl,[‡] and William R. Heineman*,[†]

[†]Department of Chemistry, University of Cincinnati, Cincinnati, Ohio 45221-0172, United States
[‡]Sustainable Carbon NanoTechnology and Engineering LLC, 7278 North U.S. Route 68, Wilmington, Ohio 45177, United States

**S** *Supporting Information*

**ABSTRACT:** A Nafion film loaded with novel catalyst-free multiwalled carbon nanotubes (MWCNTs) was used to modify a glassy carbon (GC) electrode to detect trace concentrations of metal ions, with europium ion ($Eu^{3+}$) as a model. The interaction between the sidewalls of MWCNTs and the hydrophobic backbone of Nafion allows the MWCNTs to be dispersed in Nafion, which was then coated as a thin film on the GC electrode surface. The electrochemical response to $Eu^{3+}$ was found to be ~10 times improved by MWCNT concentrations between 0.5 and 2 mg/mL, which effectively expanded the electrode surface into the Nafion film and thereby reduced the diffusion distance of $Eu^{3+}$ to the electrode surface. At low MWCNT concentrations of 0.25 and 0.5 mg/mL, no significant improvement in signal was obtained compared with Nafion alone. Scanning electron microscopy and electrochemical impedance spectroscopy were used to characterize the structure of the MWCNT−Nafion film, followed by electrochemical characterization with $Eu^{3+}$ via cyclic voltammetry and preconcentration voltammetry. Under the optimized conditions, a linear range of 1−100 nM with a calculated detection limit of 0.37 nM (signal/noise = 3) was obtained for determination of $Eu^{3+}$ by Osteryoung square-wave voltammetry after a preconcentration time of 480 s.
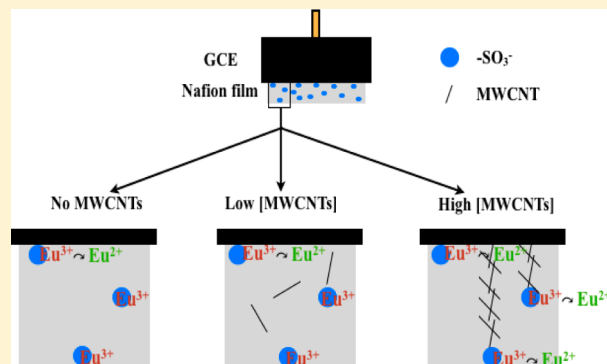
**C**arbon nanotubes (CNTs) have become a widely studied carbon material since their discovery.[1] The unique structural, chemical, and electronic characteristics as well as chemical stability have led to useful applications of this material in electrochemistry.[2] Many chemical sensors, supercapacitors, and optical and electronic devices have been developed that use CNTs.[3−5] Laser ablation, arc discharge, and, most commonly, chemical vapor deposition are the main techniques currently used for CNT fabrication.[6] However, all of those processes inevitably involve use of metal catalysts, which may be retained in the CNTs and interfere with their electrochemical behavior.[7] In order to eliminate interference from residual metal catalyst, catalyst-free single-walled CNT disk electrodes were produced through a carbo-thermal carbide conversion (CTCC) method. These electrodes exhibited good sensitivity and selectivity when they were applied to sensing organic compounds and heavy metals.[8,9] Besides this, catalyst-free multiwalled carbon nanotubes (MWCNTs) were fabricated by the CTCC method and deposited on basal-plane pyrolytic graphite, which also exhibited good electrochemical properties.[10]

Nafion is a synthetic ionomer generated by polymerization of perfluorinated vinyl ether and tetrafluoroethylene backbone and terminated with sulfonic acid.[11] It has been widely used in applications of fuel cell fabrication, sensor development, and organic synthesis because of its chemical and thermal stability and high cation conductivity.[12−15] In sensor development, a Nafion-modified electrode can be easily prepared by coating with a Nafion solution followed by solvent evaporation from the electrode, and its sulfonate group can selectively preconcentrate cations while serving as a barrier against anions.[16,17]

It is known that hydrophobic−hydrophobic interactions between the sidewalls of CNTs and the fluorocarbon backbone of Nafion can allow the dispersion of CNTs in Nafion, which enables the immobilization of solid/powder like CNTs on an electrode surface.[18] When immobilized on an electrode surface, CNTs and Nafion play different roles in response to an analyte. However, the mechanism of CNT concentration-dependent electrochemical performance has not been thoroughly studied and it is important to unravel this mechanism.

Europium is one of the most reactive rare earth elements.[19] It has many important applications in industry, materials science, and life sciences due to its unique electronic and optical properties.[20] With the increasing use of europium, continuous exposure to it is a concern for potential health issues, yet few regulations have been proposed to monitor europium levels in industry.[21] To date, commonly applied techniques for trace europium determination (mainly through the detection of
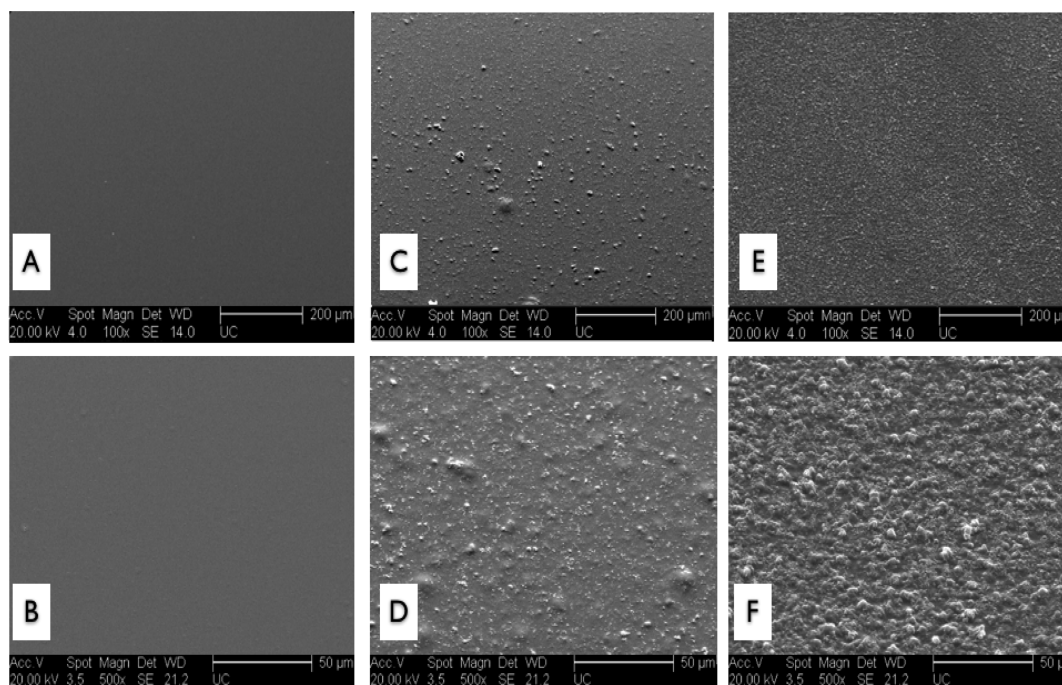
**Figure 1.** SEM images of (A, B) Nafion-modified GC electrode and (C, D) 0.25 mg/mL and (E, F) 2 mg/mL MWCNT−Nafion modified GC electrode at (A, C, E) 100× and (B, D, F) 500× magnification.

$Eu^{3+}$) are inductively coupled plasma atomic mass spectrometry, graphite furnace and tungsten coil electrothermal atomic absorption spectrometry, UV−vis absorption spectrophotometry, and luminescence.[22−25] Although quite sensitive and accurate, those techniques typically require sample pretreatment and expensive apparatus.

Electrochemical techniques are important for detecting metals because of their low cost, high sensitivity, selectivity, and efficiency. The deposition step in anodic stripping voltammetry techniques can effectively accumulate trace-level metal ions from the bulk solution at the electrode surface in the form of metal atoms by applying a reduction potential. After that, the potential is scanned positively, causing the metal to be reoxidized to ions, and the anodic peak current generated can be quantitatively related to the metal ions in the analyte.[26] Chemically modified electrodes can also be exploited to preconcentrate analyte of interest through a selective interaction between the electrode and the analyte prior to voltammetric quantitation.[27] Until now, two main electrochemical preconcentration methods have been developed for europium sensing through the reduction of $Eu^{3+}$ to $Eu^{2+}$: mercury electrode-based adsorptive stripping voltammetry and Nafion-modified electrode-based preconcentration voltammetry.[28−31] Also, recent work using a $LaB_6$ electrode in conjunction with the surfactant sodium dodecylbenzenesulfonate has been reported to sensitively detect $Eu^{3+}$ by differential pulse voltammetry.[21]

Here we introduce catalyst-free MWCNTs produced by the CTCC process incorporated in a Nafion film on a glassy carbon (GC) electrode and explore its application to preconcentration voltammetry with $Eu^{3+}$ as a representative metal ion. In addition to its importance described above, we chose $Eu^{3+}$ because of our interest in developing sensors for metals used to alloy magnesium to form biodegradable metal implants.[32] Through the electrostatic attraction with the sulfonate group of Nafion, $Eu^{3+}$ can be preconcentrated in the MWCNT−Nafion

film on a GC electrode as the sensor. The surface of the sensor was first characterized by scanning electron microscopy (SEM). The mechanism of MWCNT concentration-dependent electrochemical performance was studied by electrochemical impedance spectroscopy (EIS). The sensor was then applied to $Eu^{3+}$ preconcentration via cyclic voltammetry and Osteryoung square-wave voltammetry.

## EXPERIMENTAL SECTION

**Reagents.** Catalyst-free MWCNTs were made as previously reported.[8,33] All chemicals and reagents were purchased from Sigma−Aldrich and used without further purification. Deionized water was used for preparing all solutions (Nanopure water purification system).

**Instrumentation.** SEM images of the sensor surface were taken with an XL30 ESEM TMP (FEI Co.) at an acceleration voltage of 20 KV. Gold was coated (10−20 $\mu$m thickness) on the sensor surface before images were taken to improve conductivity of the MWCNT−Nafion film surface. EIS was performed with a Gamry Reference 600 (Gamry Inc.). The direct current (dc) potential was set at −700 mV in experiments involving $Eu^{3+}$ in acetate buffer (pH 4.5) and −200 mV in experiments involving acetate buffer alone, with a perturbation potential of 5 mV for both solutions. The frequency range was set from 100 000 to 0.1 Hz. Cyclic voltammetry and preconcentration voltammetry (Osteryoung square-wave voltammetry technique) were performed on a BASi 100B electrochemical analyzer (BASi). In cyclic voltammetry, an initial negative scan between −200 and −1000 mV at 50 mV/s was conducted, unless otherwise stated. A 15 mL electrochemical cell (BASi) was equipped with a GC electrode (bare or modified) working electrode, Ag/AgCl (3 M KCl) reference electrode, and Pt wire auxiliary electrode.

**Electrode Preparation.** Prior to use, the GC electrode was polished with 0.05 $\mu$m alumina on a polishing cloth (Catalog no. 40-7218, Buehler Co.) and cleaning bath ultrasonicated in
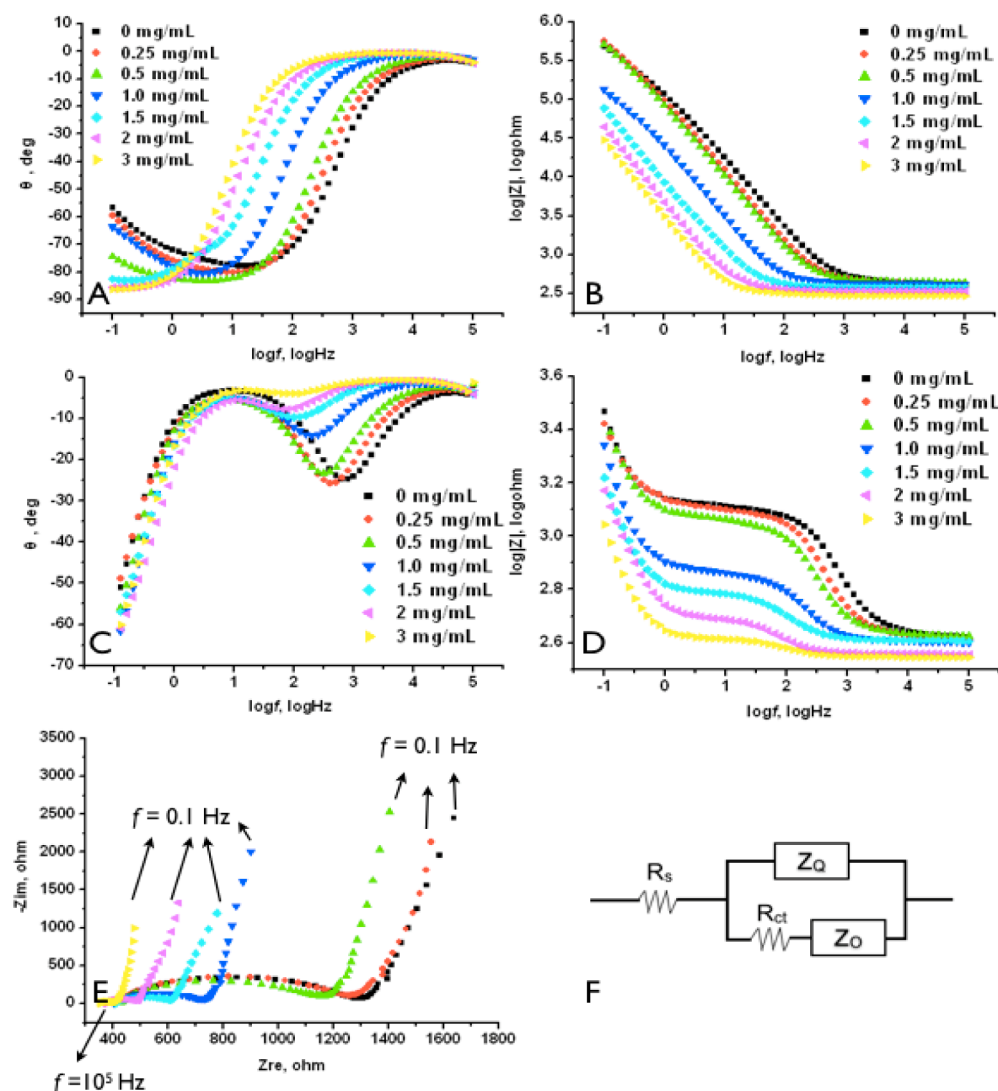
**Figure 2.** (A, B) Bode plots of 0.1 M acetate buffer, pH 4.5, with MWCNT−Nafion-modified GC electrode. (C, D) Bode plots and (E) Nyquist plot of 1 mM Eu$^{3+}$ in 0.1 M acetate buffer with MWCNT−Nafion-modified GC electrode. (F) Equivalent circuit for the MWCNT−Nafion-modified GC electrode.

doubly distilled H$_2$O for 5 min. After being rinsed with doubly distilled H$_2$O, the GC electrode was dried with compressed air and ready to use. Different concentrations of MWCNTs (mg/mL) were mixed with 2.5% Nafion (w/v, diluted with methanol) in small glass vials and clean bath ultrasonicated until the MWCNTs were fully dispersed (about 10−30 min depending on the concentration of MWCNT). Then 5 or 15 μL of the mixture was pipetted onto the GC electrode and was allowed to evaporate in air prior to all electrochemical experiments. KCl (3 M) was used to exchange preconcentrated Eu$^{3+}$ from MWCNT−Nafion film to recycle the modified electrode for the next experiment.

## ■ RESULTS AND DISCUSSION

**Scanning Electron Microscopy.** Visualizing the MWCNT−Nafion film on the GC surface by SEM proved very useful in optimizing the procedure for preparing reproducible sensors. Initial attempts to form films gave irreproducible electrochemical results. The key to improved performance was to thoroughly mix and sonicate the MWCNT−Nafion mixture before it was applied to the GC

electrode surface. Coating with Nafion alone formed a thin, smooth film on the GC electrode surface as shown by the SEM images at 100× and 500× magnification in Figure 1 panels A and B, respectively. The thickness of the films was ∼20−30 μm. After addition of 0.25 mg/mL MWCNTs, the smooth Nafion-coated surface became rough, showing a scattered distribution of MWCNT clusters that were separated by Nafion, as can be seen in Figure 1C,D. Increasing the concentration of MWCNTs to 2 mg/mL gave a much rougher surface with a dense but even distribution of MWCNT clusters throughout the Nafion, as shown at two magnifications in Figure 1E,F. Insufficient mixing/sonication gave films with very irregular aggregation of the MWCNTs as compared to the relatively even distribution. As previously reported by Banks and co-workers,[10] using transmission electron microscopy, the MWCNTs are 150 (±50) nm in length and between 6 and 10 graphite layers thick. The roughness shown in Figure 1E,F is clearly due to aggregation of the MWCNTs into clusters, since individual MWCNTs are too small to be seen by SEM. As shown in Figure 1F, the aggregates are of size 5 μm and smaller. Attempts to further disperse the MWCNTs into smaller

aggregates were unsuccessful. However, MWCNT−Nafion prepared in this way showed dramatic improvement in electrochemical performance compared to less sonicated MWCNT−Nafion, and this procedure was used for subsequent experiments. Most importantly, low concentrations of MWCNTs form clusters that are isolated from each other by Nafion and therefore not in electrical contact with each other, whereas high concentrations give a denser matrix of clusters that are most likely electrically contacting each other and thereby forming an extension of the underlying GC electrode surface.

**Electrochemical Impedance Spectroscopy.** Electrochemical impedance spectroscopy (EIS) proved very useful for studying the effect of MWCNT concentration in the Nafion film and its effect on the voltammetry of $Eu^{3+}$. EIS is a powerful technique for obtaining information about the interfacial properties of an electrode surface, such as heterogeneous charge-transfer resistance at the interface, solution resistance, and double layer structure.[34] For ionomer coatings such as Nafion, charge propagation is mainly achieved through the movement of ions or electron self-exchange between nearby ions inside the film when the loading of the redox active ions is sufficiently high to allow this "communication".[35,36] In the presence of MWCNTs, the situation in terms of electron transfer changes because of the high electronic conductivity of MWCNTs and large surface area, which reduces the diffusion distance of electroactive ions that preconcentrate into the film. So, in order to study the characteristics of the coated film, a series of EIS experiments was performed with pure Nafion (2.5%) and different concentrations of MWCNT−Nafion-modified GC electrodes in the following solutions: (1) 0.1 M acetate buffer; (2) a negatively charged redox probe that the film would be expected to reject, $Fe(CN)_6^{3-}$ in 0.1 M acetate buffer; and (3) the positively charged analyte of interest that the film would be expected to preconcentrate, $Eu^{3+}$ in 0.1 M acetate buffer. As seen in Figure 2A for acetate buffer, at high frequencies where a near-zero phase shift ($\theta$) was obtained, the electrode behaves primarily as a resistor due to the solution/film resistance.[37] At intermediate frequencies with the appearance of capacitive behavior, the imaginary component of the impedance ($Z_{im}$) became significant, where $\theta$ started to increase.[37] Impedance information can also be obtained from another form of the Bode plot as shown in Figure 2B. The plateaus at higher frequencies correspond to resistance of the solution, and the lines at intermediate and low frequencies are associated with capacitive impedance.[18]

As indicated by the Bode plots, low concentrations of 0.25 and 0.5 mg/mL MWCNTs showed no significant difference in |Z| compared with Nafion alone, whereas from 1 to 3 mg/mL a rather abrupt shift to smaller |Z| and larger capacitance ($Z = -j/\omega C$; where $j^2 = -1$, $\omega$ is the angular frequency, and $C$ is the capacitance) occurs, suggesting that the concentration of MWCNTs plays an important role in this process above a certain threshold level. Furthermore, with higher concentrations of MWCNTs at 2 mg/mL (purple) and 3 mg/mL (yellow), the near 0° phase shift at high frequencies and near −90° shift at low frequencies, as well as the single break point (corner point) in log |Z| versus log $f$ Bode plot shown in Figure 2D, compared with Figure 2B, imply a case of primarily capacitive behavior of the electrode existing at those MWCNT concentrations.[37] The similarity of the Bode plots in the presence (Figure S1, Supporting Information) and absence of $Fe(CN)_6^{3-}$ (Figure 2A,B) suggests that 2.5% Nafion

completely blocks the diffusion of negatively charged $Fe(CN)_6^{3-}$ from the bulk solution into the film and to the underlying electrode, which was confirmed by cyclic voltammetry, where no reduction−oxidation current was observed for $Fe(CN)_6^{3-}$ (data not shown) under the same conditions.

However, when the analyte is switched to $Eu^{3+}$, preconcentration of $Eu^{3+}$ in the film occurs due to electrostatic attraction between the negative sulfonate group of Nafion and $Eu^{3+}$, which caused very different EIS responses compared to those for the acetate buffer and $Fe(CN)_6^{3-}$. Figure 2C,D shows Bode plots for the MWCNT−Nafion-modified GC electrode in response to 1 mM $Eu^{3+}$. Similar to Figure 2A, a near 0° $\theta$ at high frequencies was obtained in the presence of $Eu^{3+}$ because of the solution resistance, whereas at intermediate frequencies, charge transfer between MWCNT−Nafion and the preconcentrated $Eu^{3+}$ occurred, showing well-defined peaks (Figure 2C).[18] In the log |Z| versus log $f$ Bode plot shown in Figure 2D, compared with Figure 2B, a second plateau and traces with smaller log |Z| values at intermediate to low frequencies were found, which indicated restricted diffusion of $Eu^{3+}$ within the film (Figure 2D).[18,37]

A more commonly used plot in electrochemical literature, Nyquist plots, were also obtained and are displayed in Figure 2E. The Nyquist plot includes semicircular and linear parts. The semicircular part at high frequencies is associated with the charge-transfer process, and the linear part at lower frequencies results from capacitive behavior of the finite thickness diffusion impedance.[21] It can be seen that depressed semicircles and typical angles between 45° and 90° exist for the linear region with respect to the $Z_{re}$ and $Z_{im}$ axes, indicating that a nonideal capacitor known as constant phase element (CPE) is present (Figure 2E).[18,38] CPE is generally considered to originate from the distribution of double layer capacitance along the electrode interface as a result of surface inhomogeneity, which in this case should be due to the roughness of the MWCNT modification.[39] A model equivalent circuit (Figure 2F) adapted from a previous study was found to most adequately fit the EIS data.[21] It contains the solution resistance ($R_s$), which contains the resistance of the supporting electrolyte and the film (Nafion alone or MWCNT + Nafion) resistance, the charge-transfer resistance of the electrochemical reaction of the redox couple ($R_{ct}$), the CPE corresponding to the double layer capacitance ($C_{dl}$) of the electrode ($Z_Q$), and the finite thickness Warburg diffusion impedance of $Eu^{3+}$ for the electrode ($Z_O$). More details of the model equivalent circuit are included in Supporting Information. The fitting values of the parameters are summarized in Table S1 (Supporting Information). The overall decrease of $R_s$ is due to the decrease of film resistance upon adding MWCNT in the Nafion. It was reported previously that the semicircle of the Nyquist plot results from two charge-transfer processes: electron transfer between the electron conductor and the redox species, and ion transfer across the interface of the film.[18] As the concentration of MWCNTs increases from 1 to 3 mg/mL, the diameter of the semicircles ($R_{ct}$) in the Nyquist plots dramatically decreases. However, at lower concentrations of MWCNTs, no significant change of charge-transfer resistance was obtained in 0.25 mg/mL MWCNTs compared with the Nafion-coated electrode, and only a slight decrease of the semicircle was seen in 0.5 mg/mL MWCNTs. Thus, reduction of the charge-transfer resistance begins when a critical concentration of the MWCNTs is reached, which results from increased electron

transfer rate within the film and lowered energy barrier for ion transfer across the interface.[18]

A diagram regarding this MWCNT concentration-dependent mechanism is proposed in Scheme 1. In the absence of

## Scheme 1. Mechanism of MWCNT Concentration-Dependent Effects
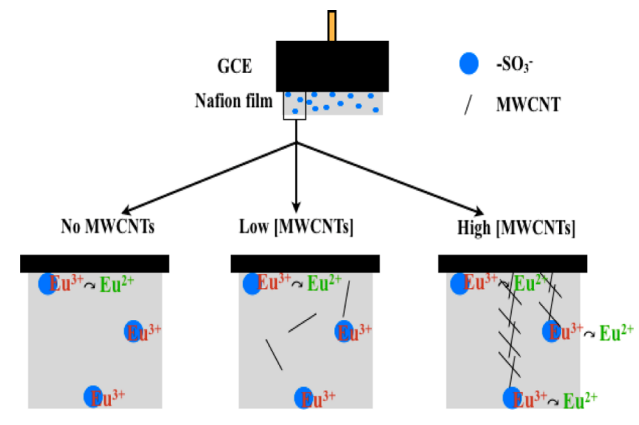


MWCNTs (left electrode), $Eu^{3+}$ concentration is enhanced at the GC electrode surface through ionic attraction with Nafion, where electron transfer is achieved by diffusion of $Eu^{3+}$ to the GC electrode surface, where it is reduced to $Eu^{2+}$. When low concentrations of MWCNTs are present, few interconnections are established among individual nanotubes or nanotube clusters, which was also seen in the SEM images (Figure 1C,D), where a scattered MWCNT distribution was obtained at low concentrations of MWCNTs. Thus, no significant increase in the microscopic surface area of the electrode surface is caused by the presence of MWCNTs, and the electron-transfer rate is comparable to that of Nafion alone. Thus, the same diffusion distance across the film and charge-transfer mechanism occurs as with only Nafion present. When MWCNT concentrations increase to a "critical point", the individual nanotubes (or clusters) begin to connect, which was also seen in SEM images (Figure 1E,F), where the MWCNTs are in contact with each other and thereby extend the electrode surface into the Nafion film, which significantly increases the microscopic surface area of the electrode. This enables electron transfer to now occur within the film, which reduces the diffusion distance. Instead of happening only at the GC electrode surface, the reduction of $Eu^{3+}$ to $Eu^{2+}$ now also occurs at both the underlying GC electrode surface and the MWCNT matrix within the film, as illustrated in Scheme 1 (right electrode). In order to confirm this mechanism, further investigations with cyclic voltammetry and preconcentration voltammetry were carried out.

**Cyclic Voltammetry.** The electrochemical behavior of the MWCNT−Nafion-modified electrode was then investigated by cyclic voltammetry (CV). The background CVs in acetate buffer containing primarily capacitance current are shown in Figure 3. As seen in Figure 3, the presence of Nafion produces about the same capacitance current as the bare GC electrode, whereas when 1 mg/mL and greater concentrations of MWCNTs are mixed in, the capacitance current dramatically increases, as would be expected if the microscopic electrode surface is significantly increased in the film by formation of a conducting matrix of MWCNTs. The large capacitive current for the MWCNT-modified electrode indicates good charge
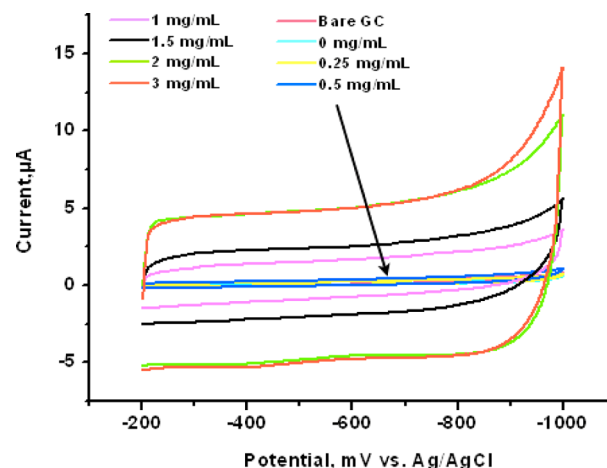


**Figure 3.** Cyclic voltammetry of bare GC electrode, Nafion-coated GC electrode, and 0.25−3 mg/mL MWCNT−Nafion-modified GC electrode in 0.1 M acetate buffer, pH 4.5, at a scan rate of 50 mV/s.

propagation within the electrode as a result of electrochemical double layer capacitance, which is generated at the electrode (Nafion)/electrolyte interface and determined by the effective surface of the electrode and dielectric constant of the electrolyte.[39] Although not designed to be a capacitor, it is still interesting to investigate the specific capacitance ($C_s$) of this electrode after MWCNT modification (detailed calculation of $C_s$ is available in Supporting Information). Herein, $C_s$ of this typical MWCNT-modified GC electrode is 3.4 F/g, which is about the same as the superaligned carbon nanotubes used in a supercapacitor before metal oxide treatment.[4]

Comparison of the capacitance currents with various concentrations of MWCNTs also showed that the magnitudes of the currents were dependent on MWCNT concentrations (Figure 3): similar small-capacitance currents were obtained with low concentrations of MWCNTs (0, 0.25, and 0.5 mg/mL), while much larger capacitive currents were exhibited for higher concentrations of MWCNTs. This agrees well with the MWCNT concentration-dependent electrochemical results for EIS described above and the mechanism proposed in Scheme 1.

To further characterize the electrode, the effect of scan rate on CV behavior of the MWCNT-omodified electrode was performed with 1 $\mu$M $Eu^{3+}$ after preconcentration for 480 s. Various scan rates from 5 to 500 mV/s were applied at a 2 mg/mL MWCNT−Nafion-modified GC electrode. The voltammograms in Figure 4 display well-defined voltammetric waves as well as near-equal anodic and cathodic peaks at those scan rates. At the slowest scan rate of 5 mV/s, the voltammograms were distinctly thin layer in appearance (restricted diffusion), with a peak separation of 17 mV and currents dropping rapidly to background after the peak, as shown by the inset in Figure 4. The peak separation systematically increased from 17 to 65 mV as the scan rate increased from 5 to 50 mV/s. The near-symmetric cathodic and anodic currents increased linearly with scan rate, and the current continued to drop back to the background after reaching the peaks. However, at scan rates larger than 100 mV/s, peak separations increased up to 205 mV (500 mV/s), the current no longer dropped to background after the peak, and the peak currents were no longer linearly correlated with the scan rate but were proportional to the square root of scan rate [Figure 4 (inset) and Figure S2, Supporting Information]. This phenomenon suggests that, for $Eu^{3+/2+}$, there is a conversion from restricted diffusion thin layer
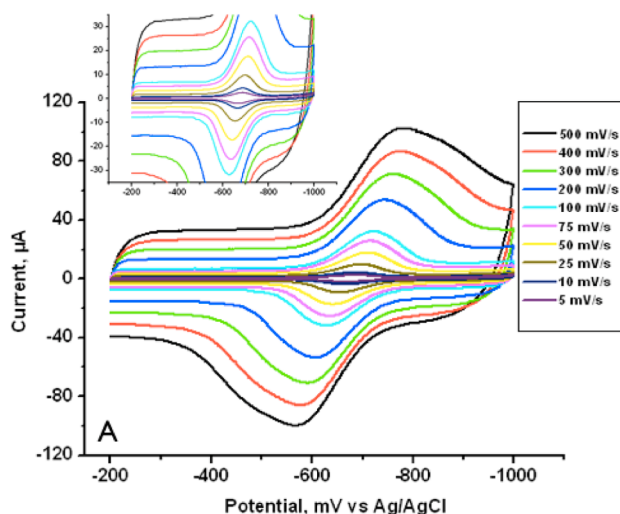
**Figure 4.** Scan rate study of Eu³⁺ at 2 mg/mL MWCNT−Nafion-modified GC electrode. (Inset) Zoomed view of CVs at slower scan rates.

electrochemical behavior at lower scan rates to semi-infinite diffusion-controlled electrochemical response at higher scan rates. At the Nafion-alone GC electrode, peak separations varied from 32 mV (5 mV/s) to 260 mV (500 mV/s), much larger than the 2 mg/mL MWCNT−Nafion-modified GC electrode. This behavior is consistent with Scheme 1 where, at high concentrations of MWCNTs (2 mg/mL), the diffusion distance is greatly decreased by MWCNTs, where the microscopic surface area is extended throughout the Nafion film by the connection of individual nanotubes or clusters, resulting in a restricted diffusion surface-confined redox process for Eu³⁺/²⁺ at lower scan rates.

**Electrode Recycling, pH, MWCNT Concentration, and Preconcentration Time Effects on Eu³⁺ Electrochemistry.** In order to recycle the modified film, the electrode was immersed in different concentrations of KCl to remove Eu³⁺. With low KCl concentration between 0.1 and 0.5 M, the modified film cannot be recovered to its original condition even with an immersion time of 1 h. However, when 3 M KCl was used, most modified films can be recovered in 5−10 min

depending on the concentrations of Eu³⁺ to which they had been exposed.

Previous studies have shown that pH influences the electrochemical sensing of Eu³⁺ in that either too-low or too-high pH causes a decrease in the signal, probably due to H⁺ competition with Eu³⁺ in binding the sulfonate group of Nafion at low pH and hydrolysis of Eu³⁺ to form neutral Eu(OH)₃ at high pH.[31] By varying the pH of acetate buffer for 1 μM Eu³⁺ and using preconcentration voltammetry, very similar peak currents were obtained at pH 3.5, 4, and 4.5, whereas much lower signals were obtained at pH 3 and 5. As a result, pH 4.5 was chosen for the supporting electrolyte.

Other critical factors, including preconcentration time and concentration of MWCNTs, were studied to find optimized conditions for Eu³⁺ detection. Generally, longer preconcentration time would allow more analyte to concentrate in the film, and more MWCNTs in the Nafion would enlarge the electrode surface area and reduce the diffusion distance for Eu³⁺. Figure S3 (Supporting Information) shows the preconcentration voltammetry response to combinations of 0.25, 0.5, 1, 1.5, 2, and 3 mg/mL MWCNTs at preconcentration times of 60, 120, 180, 240, 300, 360, 420, 480, 540, and 600 s with 1 μM Eu³⁺. At lower concentrations of MWCNTs of 0.25 and 0.5 mg/mL, peak currents remained relatively small and reached the highest peak currents around 480∼540 s. It is noteworthy that no significant differences of the signals were obtained at 0.25 and 0.5 mg/mL MWCNTs, which is also consistent with the hypothesis that when the MWCNT concentration is too low, no connections are established among nanotubes so the electrode surface area is not extended into the film, resulting in the same diffusion distance as for Nafion alone. In contrast, when the MWCNT concentration is at 1 mg/mL and higher (particularly at 2 mg/mL), dramatic increases in peak current were observed; the overall highest response was obtained at 480 s. When the MWCNT concentration increased to 3 mg/mL, irreproducible peak current was obtained that was much less stable than at lower MWCNT concentrations. One possible explanation for this phenomenon is that, with higher concentrations of MWCNT, different sizes of MWCNT aggregates may form and result in less evenly distributed MWCNT in Nafion compared to lower concentrations, which then causes a less reproducible preconcentration voltammetry response. As a result, 2 mg/mL MWCNTs and 480 s were
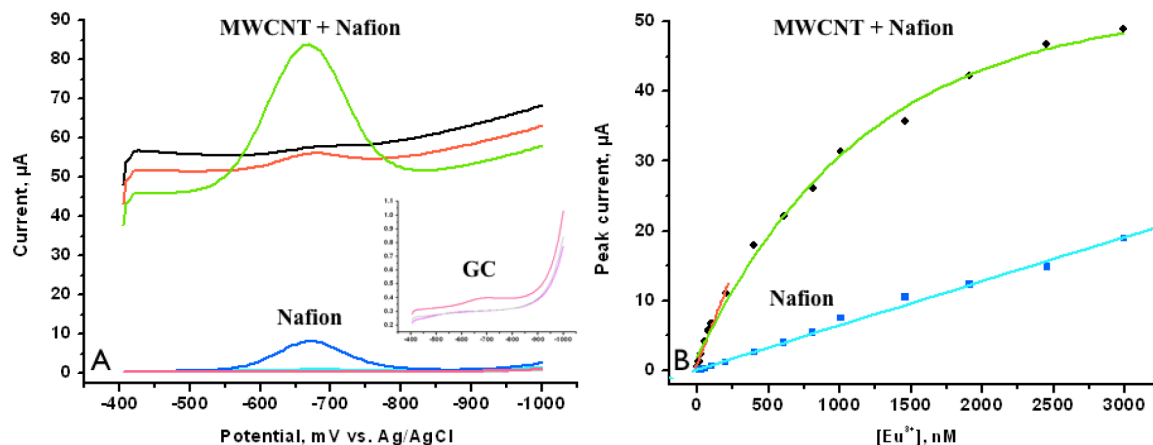


**Figure 5.** (A) Preconcentration voltammetry at bare, Nafion-modified, and 2 mg/mL MWCNT−Nafion-modified GC electrodes for 1 nM, 25 nM, and 1 μM Eu³⁺. (B) Response to concentrations of Eu³⁺ in 0.1 M acetate buffer, pH 4.5, at preconcentration time of 480 s with Nafion-coated GC and 2 mg/mL MWCNT−Nafion-modified GC electrodes.

chosen as the MWCNT concentration and preconcentration time for the experiments described in the next section.

**Determination of $Eu^{3+}$ by Preconcentration Voltammetry.** The effect of MWCNTs on the quantitative determination of $Eu^{3+}$ by preconcentration voltammetry was evaluated. Signal improvements for $Eu^{3+}$ reduction wave provided by Nafion and Nafion–MWCNT (2 mg/mL) films compared to bare GC are shown by the Osteryoung square-wave voltammograms in Figure 5A. In 1 nM $Eu^{3+}$, no signal for $Eu^{3+}$ was seen at either bare or Nafion-coated GC electrode, while a distinct peak current for $Eu^{3+}$ was found with the MWCNT–Nafion-modified GC electrode. In 25 nM and 1 $\mu$M $Eu^{3+}$, MWCNT–Nafion-modified GC electrodes exhibited peak currents 12 and 5 times higher, respectively, than Nafion-modified GC electrode (Table S2, Supporting Information). The smaller improvement factor at 1 $\mu$M $Eu^{3+}$ is attributed to the Nafion film approaching saturation with $Eu^{3+}$, where smaller amounts of $Eu^{3+}$ can be loaded into the film as determined by the concentration of sulfonate ion-exchange sites. By comparison, $Eu^{3+}$ of concentration below 1 $\mu$M was undetectable at bare GC electrode and gave a peak current 1182 times lower than the MWCNT–Nafion-modified GC electrode with 1 $\mu$M $Eu^{3+}$. The detection of increasing concentrations of $Eu^{3+}$ was then carried out. A linear range was obtained at a 2 mg/mL MWCNT–Nafion-modified GC electrode from 1 to 100 nM [$Y$ (microamperes) = $(0.064 \pm 0.003)x$ (nanomolar) + $(0.6 \pm 0.2)$]. The calculated detection limit is 0.37 nM (signal/noise = 3). From $Eu^{3+}$ concentrations from 1 nM to 3 $\mu$M, a fitted curve was obtained. This curve-shaped concentration–signal response is typical for ion-exchange films where the partitioning saturation of the analyte will be reached when the ion-exchange site is saturated with analyte (Figure 5B). At the Nafion-modified GC electrode, one linear range of 16 nM~3 $\mu$M is obtained as $Y$ (microamperes) = $(0.0063 \pm 0.0002)x$ (nanomolar) + $(0.1 \pm 0.2)$ (Figure 5B). No further concentrations were studied above 3 $\mu$M since it is above the level of any $Eu^{3+}$ contamination levels.[21] This MWCNT–Nafion-modified GC electrode shows much higher sensitivity and lower detection limit, compared with 0.002 $\mu$A/nM and 10 nM, and 0.19 $\mu$A/nM and 6 nM for recently reported $Eu^{3+}$ sensors.[18,21]

## CONCLUSIONS

A MWCNT–Nafion-modified GC carbon electrode was developed for sensitive detection of $Eu^{3+}$. EIS, cyclic voltammetry, and preconcentration voltammetry were applied to study the MWCNT concentration-dependent electrochemical behavior of the modified electrode. In EIS, the constant decrease in solution and charge-transfer resistances with increasing MWCNT concentrations above 0.5 mg/mL and no significant difference in resistance at 0.25 mg/mL indicates a specific role of MWCNTs in changing resistance. The interconnection of individual nanotubes is considered as the key factor in this process. Cyclic voltammetry and preconcentration voltammetry further confirmed this hypothesis because the increase of capacitance currents in CV and the dramatic improvement of peak currents in response to $Eu^{3+}$ happens only when MWCNT concentrations are higher than 0.5 mg/mL, while low MWCNT concentrations of 0.25 and 0.5 mg/mL MWCNTs exhibit similarly low signals. Additionally, the scan rate studies have shown that $Eu^{3+}$ reduction at the modified electrode is a restricted diffusion process at slow scan rate where the small diffusion distance is the result of individual connection of nanotubes that enable direct electron transfer at the MWCNTs.

Besides $Eu^{3+}$, this type of sensor could be used for sensing other metal ions that have at least two stable oxidation states and are electrochemically active, such as $Mn^{3+}/Mn^{2+}$, $Co^{3+}/Co^{2+}$, $Ce^{4+}/Ce^{3+}$, and $Fe^{3+}/Fe^{2+}$. Also, surfactants could be used in the film to enhance preconcentration of metal ions, which could further improve the detection limit to subtrace concentrations.

Besides being applied to construction of metal ion sensors, this type of MWCNTs can also be used as electrode material to construct electrodes such as microsensors where, compared to regular electrodes, small current signal is usually seen because of the size limitation of the microsensor. The use of MWCNTs can help overcome this issue by amplifying the signal through its large surface area to give larger, more easily measured peak currents.

## ASSOCIATED CONTENT

### Ⓢ Supporting Information

Additional information includes text describing mathematical expressions of components in model equivalent circuit and calculations of specific capacitance; three figures showing Bode plots of MWCNT–Nafion-modified GC electrode with $Fe(CN)_6^{3-}$ and scan rate study and optimization of preconcentration time for 2 mM MWCNT–Nafion-modified GC electrode; and two tables listing fitting values of components in model equivalent circuit and representative peak current vs concentration of $Eu^{3+}$ at different electrodes. This material is available free of charge via the Internet at http://pubs.acs.org/.

## AUTHOR INFORMATION

### Corresponding Author
*Telephone 01-513-556-9210; fax 01-513-556-9239; e-mail William.Heineman@uc.edu.

### Notes
The authors declare the following competing financial interest(s): Bill L. Riehl declares a financial interest in Sustainable Carbon Nano Technology and Engineering LLC.

## ACKNOWLEDGMENTS

## REFERENCES

(1) Iijima, S. *Nature* **1991**, *354*, 56−58.
(2) Pastorin, G. *Carbon Nanotubes: From Bench Chemistry to Promising Biomedical Applications*; Pan Stanford Publishing: Singapore, 2011.
(3) Wang, J. *Electroanalysis* **2005**, *17*, 7−14.
(4) Zhou, R.; Meng, C.; Zhu, F.; Li, Q.; Liu, C.; Fan, S.; Jiang, K. *Nanotechnology* **2010**, *21*, 1−7.
(5) Hartschuh, A.; Pedrosa, H. N.; Peterson, J.; Huang, L.; Anger, P.; Qian, H.; Meixner, A. J.; Steiner, M.; Novotny, L.; Krauss, T. D. *ChemPhysChem* **2005**, *6*, 1−6.
(6) Sharon, M.; Sharon, M. *Carbon Nanoforms and Applications*; McGraw Hill: New York, 2010.

(7) Park, T.; Banerjee, S.; Hemraj-Benny, T.; Wong, S. S. *J. Mater. Chem.* **2006**, *16*, 141−154.

(8) Wang, T.; Manamperi, H. D.; Yue, W.; Riehl, B. L.; Riehl, B. D.; Johnson, J. M.; Heineman, W. R. *Electroanalysis* **2013**, *25*, 983−990.

(9) Yue, W.; Riehl, B. L.; Pantelic, N.; Schlueter, K. T.; Johnson, J. M.; Wilson, R. A.; Guo, X.; King, E. E.; Heineman, W. R. *Electroanalysis* **2012**, *24*, 1039−1046.

(10) Jones, C. P.; Jurkschat, K.; Crossley, A.; Compton, R. G.; Riehl, B. L.; Banks, C. E. *Langmuir* **2007**, *23*, 9501−9504.

(11) Mauritz, K. A.; Moore, R. B. *Chem. Rev.* **2004**, *104*, 4535−4585.

(12) Passalacqua, E.; Lufrano, F.; Squadrito, G.; Patti, A.; Giorgi, L. *Electrochim. Acta* **2001**, *46*, 799−805.

(13) Wang, X.; Dzyadevych, S. V.; Chovelon, J.; Renault, N. J.; Chen, L.; Xia, S.; Zhao, J. *Talanta* **2006**, *69*, 450−455.

(14) Yamato, T.; Hideshima, C.; Surya Prakash, G. K.; Olah, G. A. *J. Org. Chem.* **1991**, *56*, 2089−2091.

(15) Moilanen, D. E.; Piletic, I. R.; Fayer, M. D. *J. Phys. Chem. C* **2007**, *111*, 8884−8891.

(16) Swaile, B. H.; Blubaugh, E. A.; Seliskar, C. J.; Heineman, W. R. *Anal. Chem.* **1998**, *70*, 4326−4332.

(17) Fan, D.; Sun, J.; Huang, K. *Colloids Surf., B* **2010**, *76*, 44−49.

(18) Hu, C.; Yuan, S.; Hu, S. *Electrochim. Acta* **2006**, *51*, 3013−3021.

(19) Moreno, L. M. *Europium: Compounds, Production and Applications*; Nova Science Publishers, Inc.: New York, 2011.

(20) Kirk, O. R.; Othmer, F. D. *Kirk-Ohmer Encyclopedia of Chemical Technology*, 5th ed.; Wiley: New York, 2008.

(21) Ma, X.; Xu, Z.; Yuan, H.; He, Y.; Xiao, D.; Choi, M. M. F. *Sens. Actuators, B* **2010**, *147*, 152−158.

(22) Cai, B.; Hu, B.; Xiong, H.; Liao, Z.; Mao, L.; Jiang, Z. *Talanta* **2001**, *55*, 85−91.

(23) Silva, J. C. J.; Garcia, E. E.; Nogueira, A. R. A.; Nóbrega, J. A. *Talanta* **2001**, *55*, 847−854.

(24) Liawruangrath, S.; Sakulkhaemaruethai, S. *Talanta* **2003**, *59*, 9−18.

(25) Chen, S.; Zhao, H.; Wang, X.; Li, X.; Jin, L. *Anal. Chim. Acta* **2004**, *506*, 25−29.

(26) Strobel, H. A., Heineman, W. R. *Chemical Instrumentation: A Systematic Approach*, 3rd ed.; Wiley: New York, 1989.

(27) Kissinger, P. T., Heineman, W. R. *Laboratory Techniques in Electroanalytical Chemistry*, 2nd ed.; Marcel Dekker: New York, 1996.

(28) Abollino, O.; Aceto, M.; Mentasti, E.; Sarzanini, C.; van den Berg, C. M. G. *Electroanalysis* **1997**, *9*, 444−448.

(29) Ugo, P.; Ballarin, B.; Daniele, S.; Mazzocchin, G. A. *Anal. Chim. Acta* **1991**, *244*, 29−38.

(30) Moretto, L. M.; Brunetti, B.; Chevalet, J.; Ugo, P. *Electrochem. Commun.* **2000**, *2*, 175−179.

(31) Yuan, S.; He, Q.; Yao, S.; Hu, S. *Anal. Lett.* **2006**, *39*, 373−385.

(32) Doepke, A.; Kuhlmann, J.; Guo, X.; Voorhees, R. T.; Heineman, W. R. *Acta. Biomater.* **2013**, *9*, 9211−9219.

(33) Riehl, B. L. Ph.D. Thesis, University of Dayton, 2009.

(34) Chang, B.; Park, S. *Annu. Rev. Anal. Chem.* **2010**, *3*, 207−229.

(35) Buttry, D. A.; Anson, F. C. *J. Am. Chem. Soc.* **1983**, *105*, 685−689.

(36) Anson, F. C.; Blauch, D. N.; Savéant, J.; Shu, C. *J. Am. Chem. Soc.* **1991**, *113*, 1922−1932.

(37) Lasia, A. In *Modern Aspects of Electrochemistry*; Conway, B. E., Bockris, J., White, R. E., Eds.; Kluwer Academic/Plenum Publishers: New York, 1999; pp 143−248.

(38) Benavente, J.; Oleinikova, M.; Muñoz, M.; Valiente, M. *J. Electroanal. Chem.* **1998**, *451*, 173−180.

(39) Stoller, M. D.; Park, S.; Zhu, Y.; An, J.; Ruoff, R. S. *Nano Lett.* **2008**, *8*, 3498−3502.